# On Intlet Pressure Boundary Conditions for CT-Based Computation of $FFR_{SS}$: Clinical Measurement of Aortic Pressure

**Jincheng Liu**
Beijing University of Technology
**Xue Wang**
Beijing University of Technology
**Junling Ma**
Beijing University of Technology
**Jian Liu**
Peking University People's Hospital
**Youjun Liu** ( lyjlma@bjut.edu.cn )
Beijing University of Technology https://orcid.org/0000-0002-1307-4696

**Research**

**Keywords:** Coronary Heart Disease, Myocardial ischemia, Calculating FFR, Aortic pressure, Microcirculation resistance.

**Posted Date:** May 5th, 2021

**DOI:** https://doi.org/10.21203/rs.3.rs-414594/v1

# Abstract

**Background and Objectives:** With the development of medical imaging and computational fluid dynamics (CFD), a fast calculation method of steady-state fractional flow reserve (FFRss) based on CTA images has been applied to predict myocardial ischemia. Whilst this is a reliable non-invasive method of calculating FFR, assumptions involved in the analysis still need to be investigated for further improvement in predictive accuracy. In this study, we analyzed the influence of inlet and outlet boundary conditions on $FFR_{SS}$.

**Methods:** A clinical trial was carried out in Peking University People's Hospital. We enrolled 15 patients with coronary heart disease. All patients underwent coronary CTA examination, aortic pressure measurement and FFR catheter surgery. In order to better reflect the relationship between different entrance boundary conditions and FFRss, we used the invasive measurement of FFR as the standard, and calculated FFRss for 15 patients with coronary heart disease with different degrees of stenosis. The boundary conditions are divided into two groups: (1) pressure calculated based on physiological formula; (2) clinically measured aortic pressure. Based on the boundary conditions calculated by the physiological formula, we further studied the changes of FFRss under different coronary vasodilation responses (12%-48% baseline).

**Results:** The research results show that although the pressure difference between the two pressure boundary conditions is 15mmHg, the FFRss calculation result does not change significantly. With the change of the vasodilation state, the microcirculation resistance of the exit boundary condition gradually increased, and the calculated FFR value increased.

**Conclusions:** We found that changes in the microcirculation resistance of coronary stenoses have a huge impact on FFRss. The changes in FFRss values caused by boundary conditions are due to the overestimation of the vasodilation response. Therefore, individualizing the hyperemia state of the stenotic vessel microcirculation resistance value is an effective method to improve the calculation of FFR.


# 1. Background

According to data from the US Centers for Disease Control (CDC) and the World Health Organization [1, 2], cardiovascular disease (CVD) is the world's leading cause of death, accounting for about 30% of deaths. Coronary Artery Disease (CAD) is the most common cardiovascular disease, which can lead to myocardial ischemia and even death [3]. Coronary artery atherosclerosis occurs, coronary artery stenosis or obstruction leads to myocardial ischemia. However, anatomically, there is no absolute correlation between severe coronary artery stenosis and functional myocardial ischemia. Among the coronary arteries with moderate stenosis (diameter stenosis rate 40%-70%), only 35% of the lesions will eventually induce severe myocardial ischemia [5].

At present, f ractional flow reserve (FFR) is considered to be the "gold standard" for the clinical diagnosis of functional myocardial ischemia[6–8]. It is defined as the ratio of the maximum blood flow of the ary artery to the maximum blood flow of the

myocardium when the same coronary artery has no stenosis. Its definition can be simplified as FFR = Pd/Pa, where Pa and Pd are respectively the maximum coronary hyperemia state (need to be achieved by injecting coronary microcirculation dilatation drugs such as adenosine to achieve [9]) the average pressure of the aortic root, The average pressure of the coronary artery distal to the stenotic lesion. FFR > 0.8 indicates that the lesion does not cause significant myocardial ischemia and no intervention is required. Fame-1 and Fame-2 experiments proved that FFR is an effective diagnostic index to determine the suitability of stent therapy [10].

With the development of medical imaging and computational fluid dynamics (CFD), non-invasive computation of FFR has been developed. Based on coronary CT angiography (CTA), the method of computational fluid dynamics is used to simulate the hemodynamics in the coronary arteries, to obtain the pressure distribution in the state of coronary congestion, and then to calculate the ratio of the distal end of coronary artery stenosis to the aortic pressure. That is, the non-invasive numerical calculation of FFR (Noninvasive Fractional Flow Reserve Derived From Coronary CT Angiography, $FFR_{CT}$). $FFR_{CT}$ technology provides a new non-invasive method for the functional detection of coronary artery stenosis [11–20]. In order to further develop this technology, it is mainly to simplify it to facilitate faster calculation of FFR, and many simplified calculation methods such as QFR, CAFFR, VFFR and FFRSS (based on steady calculation) used in this research have been derived. However, any simplified FFR calculation algorithm is inseparable from the assumptions of the model. Sensitivity analysis of boundary conditions and input parameters is essential for calculating FFR.

In the measurement of clinical FFR, doctors usually need to use vasodilators (such as adenosine) to cause the expansion of blood vessels. Adenosine activates A2A receptors and causes coronary arteries to dilate, increasing the myocardial flow of healthy people by 3.5 to 4 times [21]. In the non-invasive numerical calculation of FFR, a special challenge is to simulate the maximum congestion state of blood vessels and simulate the effect of adenosine on reducing the peripheral resistance of coronary microcirculation [22]. Studies have shown that the total coronary artery resistance drops to 0.24 times the resting value of venous blood when the blood vessels are in the state of maximum congestion. At this time, 140 mg/kg/min of vascular adenosine is clinically administered. In coronary microvascular ischemic disease, the vasodilation response is reduced, and in some extreme cases, adenosine does not cause changes in resting blood vessels [21]. It is an assumption to simulate the maximum congestion state in the FFR model based on CT calculation, which changes the microcirculation resistance to 0.24 times of the original [14]. However, because the expansion ability of microvessels varies from individual to region, the resistance of microcirculation also has a certain influence on the flow rate of coronary arteries. Microvascular resistance is used as the boundary condition of the outlet in the calculation model. In the coronary circulation, the influence of calculating FFR has not been thoroughly studied. Therefore, in this study, we have also evaluated the influence of microcirculation resistance on the calculation model.

In this study, we used different entry boundary conditions to perform CFD calculation and analysis on the coronary artery model of personalized patients, and explored the impact on FFR. The influence of

# 2. Results

The display of FFR calculated according to the aortic pressure waveform obtained in clinical trials, the pressure calculated based on physiological parameters and the two boundary conditions is shown in Table 2.

Table 2
Comparison of FFR calculation between two pressure boundary conditions

| Patients | Real aorta Average pressure(mmHg) | FFRss | Based on physiological Aortic pressure (mmHg) | FFRss |
|---|---|---|---|---|
| Case 1 | 91.33 | 0.92 | 86.8 | 0.90 |
| Case 2 | 92.66 | 0.97 | 76.31 | 0.97 |
| Case 3 | 100 | 0.93 | 76.31 | 0.93 |
| Case 3 | 100 | 0.94 | 76.31 | 0.95 |
| Case 4 | 110.33 | 0.89 | 93.27 | 0.89 |
| Case 5 | 85.66 | 0.94 | 76.61 | 0.94 |
| Case 6 | 77 | 0.96 | 76.48 | 0.96 |
| Case 7 | 98.33 | 0.96 | 76.28 | 0.96 |
| Case 8 | 96 | 0.93 | 98.88 | 0.93 |
| Case 9 | 106.66 | 0.85 | 73.62 | 0.87 |
| Case 10 | 106.66 | 0.9 | 87.17 | 0.9 |
| Case 11 | 130 | 0.93 | 104.01 | 0.94 |
| Case 12 | 96.66 | 0.96 | 75.39 | 0.96 |
| Case 13 | 100.66 | 0.78 | 91.72 | 0.79 |
| Case 14 | 91.33 | 0.94 | 82.63 | 0.94 |
| Case 15 | 93.33 | 0.97 | 92.89 | 0.97 |

Table 2 gives a quantitative comparison of the FFR values of the two boundary conditions. It can be seen that there is a good correlation with the clinical FFR, and the FFR calculated by the two boundary conditions is basically the same, which shows that the boundary conditions are calculated based on the physiological formula FFR has good accuracy. We also listed the FFR cloud image of each patient to observe the pressure changes of each patient's stenotic vessels under different boundary conditions. As shown in Fig. 6.

As different patients grow older, the state of vasodilation of blood vessels will change. In calculating FFR, we simulated three different sets of changes in the maximum congestion state (under the boundary conditions calculated based on the physiological formula), respectively calculated the calculated FFR of 15 patients in these three cases, and compared with the clinical FFR. Table 3 lists the influence of microcirculation resistance and flow rate changes on the FFR value under different conditions.

Table 3
The FFR value of 15 patients after the change of microcirculation resistance, and the change of stenosis vessel flow.

| | Microcirculation resistance 24% (baseline) | Microcirculation resistance 48% | Microcirculation resistance 72% | Stenotic blood flow 24% (baseline) | Stenotic blood flow 48% | Stenotic blood flow 72% |
|---|---|---|---|---|---|---|
| Case 1 | 0.85 | 0.94 | 0.96 | 0.69 | 0.51 | 0.46 |
| Case 2 | 0.97 | 0.99 | 0.99 | 0.05 | 0.02 | 0.01 |
| Case 3 | 0.93 | 0.96 | 0.98 | 0.28 | 0.23 | 0.20 |
| Case 3 | 0.95 | 0.97 | 0.98 | 0.27 | 0.15 | 0.11 |
| Case 4 | 0.87 | 0.88 | 0.90 | 0.36 | 0.77 | 0.55 |
| Case 5 | 0.94 | 0.97 | 0.98 | 0.11 | 0.06 | 0.07 |
| Case 6 | 0.94 | 0.95 | 0.97 | 0.39 | 0.26 | 0.19 |
| Case 7 | 0.93 | 0.95 | 0.95 | 0.11 | 0.17 | 0.11 |
| Case 8 | 0.93 | 0.94 | 0.94 | 0.31 | 0.36 | 0.25 |
| Case 9 | 0.87 | 0.92 | 0.95 | 0.15 | 0.14 | 0.13 |
| Case10 | 0.9 | 0.98 | 0.98 | 0.34 | 0.22 | 0.17 |
| Case 11 | 0.94 | 0.97 | 0.98 | 0.47 | 0.28 | 0.13 |
| Case 12 | 0.96 | 0.98 | 0.99 | 0.16 | 0.14 | 0.11 |
| Case 13 | 0.79 | 0.88 | 0.93 | 0.75 | 0.72 | 0.65 |
| Case 14 | 0.94 | 0.95 | 0.96 | 0.24 | 0.30 | 0.28 |
| Case 15 | 0.97 | 0.97 | 0.98 | 0.17 | 0.13 | 0.12 |
| Figure | | | | | | |

## 3. Discussion

With the development of medical images and fluid dynamics, the physiological calculations of coronary arteries have developed rapidly. The evaluation of myocardial ischemia based on the coronary artery function of CT images has become the mainstream of the development of coronary physiology. Any CT-based calculation model is inseparable from the discussion of boundary conditions. Taylor et al. discussed the effects of coronary imaging quality, segmentation uncertainty, blood viscosity, etc. on FFR [23], and did not conduct a detailed study on the assumption of the maximum congestion state in the calculation model.

In this study, we separately discussed the sensitivity of the inflow boundary condition pressure to FFR in the calculation model and the sensitivity of the outflow boundary condition microcirculation resistance to FFR. The results show that the boundary conditions of the two pressures have almost the same effect on FFR, but the slight change in microcirculation resistance has a greater impact on FFR. Because the change of microcirculation resistance affects the flow in the stenotic blood vessel. The flow rate is an important factor affecting FFR. The higher the flow rate with the lower the FFR.

The effect of pressure on FFR is mainly due to the undetectable boundary conditions of active pressure. Therefore, we have previously adopted the assumption of aortic pressure and the physiological calculation formula based on pressure as the boundary condition of the entrance. We conducted clinical trials for verify the difference between the boundary conditions and the actual clinical boundary conditions. The results show that the FFR values calculated by the pressure boundary conditions of the two inlets have a high correlation. It can be seen from the results that in patients 9, 10, the aortic pressure calculated by the two methods has exceeded 15mmHg, but the calculated FFR value is the same.

For patients with mild stenosis (such as patients 5, 15), the pressure drop at both ends of the stenosis is also relatively small, and the difference is very small. Therefore, even if the maximum hyperemia is reached, the two different inlet pressure boundary conditions have no change in the pressure drop at both ends of the stenosis. The maximum congestion state has a great influence on the FFR calculation of severe stenosis (such as patients 10 and 13). Because the stenosis resistance generated in the maximum congestion state is greater, and the pressure drop at both ends of the stenosis is relatively large, so the calculation is larger difference.

The change of congestion state is more obvious for patients with severe stenosis. According to Poisson's law$\mathrm{P} = \mathrm{QR}$, when the stenosis remains unchanged, the increase in flow will increase the pressure drop, and the increase in resistance will also increase the pressure drop, thereby reducing FFR value. This is a simple principle of fluid mechanics. When the flow velocity in a narrow place decreases, it will lead to a high FFR. If there are any diseases in the coronary microcirculation vessels, it may lead to an increase in FFR, resulting in a decrease in blood flow. In clinical surgery, an increase in FFR can lead to false positives, leading to misdiagnosis of the patient's condition.

In patients with stable angina, 65% of women and 32% of men have mild stenosis [30], which means that there is no stenosis but myocardial ischemia has occurred. Some of these patients suffer from coronary heart disease, which leads to a mismatch

between coronary stenosis and myocardial ischemia [30]. The current CT-based FFR technology cannot best serve this part of patients, because the technology assumes the use of the greatest possible vasodilation function [14], For patients with impaired vasodilation response, the simulation will overestimate the blood flow through the stenosis, which will result in a lower value than the clinical real FFR, which will lead to a false diagnosis of myocardial ischemia.

As the patient's age status changes, the diastolic state of stenotic vessels is also affected to a certain extent. For example, patient 7, as the diastolic state changes, the FFR value no longer changes. In patient 13, FFR changed significantly with the change of vasodilation state. Daniel et al. through the post-mortem analysis of ADVIESE ii confirmed that with age, the maximum congestion state gradually decreases, and the FFR value gradually decreases [31]. Coronary microcirculation resistance has a greater impact on FFR, mainly because the change of coronary microcirculation resistance is due to the change of vascular flow. The value of microcirculation resistance quantifies the magnitude of this change.

In this study, we confirmed that different coronary microcirculation resistances have a huge impact on the calculation of FFR. Therefore, for patients who do not have coronary artery stenosis but have myocardial ischemia, it should be noted that the FFR value calculation based on CT should take into account that the maximum hyperemia change of coronary microvascular resistance may no longer be 0.24 this phenomenon. One way to solve this problem is to be able to quantify the changes in coronary microvessels in different patients, and the changes in the maximum congestion state of microcirculation resistance. In future work, we will establish the relationship between the diastolic state of microcirculation resistance and age to solve this problem. Another method is to use resting diagnostic indicators, which do not depend on the congestion state of blood vessels, such as IFR, RFR, etc. to diagnose myocardial ischemia.

The quality of the CTA image may affect the reconstruction of the 3D model, and the accuracy of the reconstruction of the coronary artery model affects the accuracy of calculating the FFR to a certain extent. On the other hand, the method of calculating FFR based on steady state mentioned in this study is a more reliable non-invasive method of calculating FFR. The model is improved based on the geometric multi-scale model [14]. This study explored the boundary conditions of the entrance and exit of the model, but did not discuss other physiological parameters in the model too much, which should be considered in the future work. What this model gives is the boundary condition of the inlet pressure. In other assumptions, the boundary condition based on the inlet flow is also considered in our future work.

# 4. Conclusions

In this study, we separately discussed the sensitivity of the entrance boundary conditions and exit boundary conditions of the non-invasive calculation FFR model based on CT images to FFR. We found that the pressure change of the inlet pressure boundary condition has no obvious effect on the results of FFRCT. The main reason for the change of FFRCT is the change of the microcirculation resistance at the

end of the blood vessel. Therefore, in future work, personalizing the patient's microcirculation resistance is an effective method to improve the calculation of FFR based on CT.

# 5. Methods

# 5.1 Enrolled patients

In cooperation with Peking University People's Hospital, we enrolled 16 blood vessels in 15 patients with stable angina pectoris for obtain true pressure aortic pressure waveform. All patients underwent 256-slice CT scan, transcatheter FFR operation, and acquired the patient's aortic pressure waveform and clinical physiological parameters during the operation. The institutional review boards of the participating centers approved the study protocol, and each patient signed an informed consent. The Biomechanics Laboratory of Beijing University of Technology analyzed the anonymized data independently. The participants' data are shown in Table 1.

Table 1
characteristic form of patients

| | Age | HR | Sex | Stenosis location | Stenosis | FFR |
|---|---|---|---|---|---|---|
| Case 1 | 62 | 48 | M | RCA | 80 | 0.89 |
| Case 2 | 66 | 70 | F | LAD | 60 | 0.84 |
| Case 3 | 58 | 75 | M | LAD | 50 | 0.84 |
| Case 3 | | | | LCX | 50 | 0.97 |
| Case 4 | 65 | 63 | M | LAD | 70 | 0.87 |
| Case 5 | 69 | 66 | M | LAD | 50 | 0.92 |
| Case 6 | 81 | 68 | M | LAD | 60 | 0.99 |
| Case 7 | 80 | 63 | F | LAD | 60 | 0.91 |
| Case 8 | 61 | 62 | F | RCA | 50 | 0.91 |
| Case 9 | 78 | 69 | F | RCA | 60 | 0.98 |
| Case 10 | 70 | 62 | M | LCX | 70 | 0.96 |
| Case 11 | 42 | 57 | M | LCX | 70 | 0.89 |
| Case 12 | 59 | 73 | F | LAD | 70 | 0.88 |
| Case 13 | 52 | 95 | M | LAD | 50 | 0.71 |
| Case 14 | 52 | 69 | M | LAD | 70 | 0.87 |
| Case 15 | 57 | 73 | M | LAD | 50 | 0.84 |
| RCA: right coronary artery, LAD: left anterior descending (artery), LCx: left circumflex. | | | | | | |
| HR: Heart rate. | | | | | | |

## 5.2 Three-dimensional reconstruction of coronary image

The resolution of the coronary artery CTA images of the enrolled patients was 512*512. The interval between adjacent CTA image slices was 1mm, and the pixel quality of each slice was 0.5 mm*0.5 mm. Nitroglycerin was administered before CT and FFR acquisition. We used a 3-D model reconstruction software to reconstruct the epicardial coronary artery model. According to the coronary artery lumen segmentation [23], the segmented coronary arteries' minimum diameter was 1mm, and coronary arteries greater than 1 mm in diameter were included. The mesh of the coronary model is divided by ANSYS software, using a tetrahedral mesh with 6 layers of prismatic elements on the boundary, and the number of meshes for a single model is 200,000. The grid sensitivity analysis of the model is carried out, and the calculation effect is the best when the grid is around 200,000.

## 5.3 Model for calculating FFR based on CT: $FFR_{SS}$

A fast calculation method of steady-state blood flow reserve based on CTA images (FFRss) [24] has been applied to the non-invasive diagnosis of myocardial ischemia. Taylor et al pioneered a non-invasive calculation of FFR based on CT [14], and we proposed a steady-state method for calculating FFR based on the calculation model. This method is a simplified version of the geometric multi-scale FFR calculation model. The specific calculation process is as follows: Construct a three-dimensional model of the coronary artery based on the patient's coronary artery CTA image. The average pressure of the aorta is used as the boundary condition of the inlet, and the microcirculation resistance calculated by the coronary flow is used as the boundary condition of the outlet. We can quickly calculate the flow rate and pressure distribution in patients with coronary congestion. The calculation structure is shown in Fig. 1.

The boundary conditions of the 3D coronary artery model are very important for numerical calculation of FFRss, and the accuracy of FFRss calculation strongly depends on the boundary conditions. The inlet boundary condition of the FFRss calculation model is based on the assumption of a physiological situation. The aortic pressure is calculated by the physiological formula of the human body. The coronary artery outlet of the model is connected with a resistance that simulates the coronary microcirculation resistance. Therefore, it is necessary to analyze the influence of the boundary conditions of the entrance and exit of the calculation model on FFRss to improve the accuracy of the calculation of the FFR model to predict myocardial ischemia.

In the solution of the FFRss calculation model, we assume that the blood vessel wall is rigid and simulate the blood flow as an incompressible viscous Newtonian fluid. The density is usually selected as 105 0kg/m3, and the dynamic viscosity is 0.0035 Pa·s. Use commercial software solver ANSYS-CFX to solve Navier-Stokes and continuity equations to obtain the distribution of coronary artery stenosis vessel pressure and flow.

# 5.4 Entry boundary condition acquisition

In the previous FFRss boundary conditions, the boundary conditions of the patient's 3D coronary entrance were set to aortic pressure (Pa), but the aortic pressure needs to be measured clinically, so we contracted based on the patient's physiological parameters provided in the literature [25] Pressure (SBP), diastolic blood pressure (DBP) and heart rate (HR) to obtain:

$$\mathrm{Pa} = \mathrm{DBP} + \left[\frac{1}{3} + (\mathrm{HR} * 0.0012) * (\mathrm{SBP} - \mathrm{DBP})\right] \qquad 2-1$$

In addition, we have obtained the real aortic pressure waveform clinically for verify the influence of the aortic pressure based on the physiological formula on the calculation of FFR. During the FFR operation, the professional clinician obtained the true aortic pressure waveform of the patient for several cycles through the pressure guide wire, as shown in Fig. 2.

We use the obtained two pressures as the boundary conditions for FFRss calculation to calculate FFR, and compare and analyze the results of the two boundary conditions calculations.

# 5.5 Simulation of microcirculation resistance at the coronary arteries

We equate the resistance of the microcirculation downstream of the coronary artery to the resistance, as the boundary condition of the coronary artery exit of the calculation model, determine the resistance according to the structure of the coronary artery [27]. According to the allometric scaling law, there is a power-law relationship between flow velocity and vessel diameter [28], and the flow velocity of each coronary artery branch can be calculated according to (2–2):

$$\mathrm{Qmn} = \frac{Dmn^{2.7} * Q}{Dm1^{2.7} + Dm2^{2.7} + \cdots + Dmn^{2.7}} (n = 1,2,..,n) \qquad 2-2$$

Qm is the total flow of coronary artery branches of the m sublevel, and Qmn is the flow of the branch n in the m sublevel, and n is the total number of branches of the m sublevel.

According to the flow of each branch of the coronary artery, based on the basic principles of electricity. Therefore, the microcirculation resistance of each coronary artery branch outlet can be obtained. The calculation formula is shown in (2–3). The schematic diagram of the calculation of coronary microcirculation resistance is shown in Fig. 3.

$$\mathrm{Rn_{res}} = \frac{Pa - Pv}{Q} \qquad 2-3$$

Rn_res represents the microcirculation afterload resistance value of the coronary artery branch n in the static state, Pv is the venous pressure of the venous blood vessel, Pa is the pressure of the coronary artery outlet, and Q is the flow of the coronary artery branch at this time.

The simulation method based on CT calculation of FFR for the simulation of the maximum vascular congestion state adopts the assumption that when the blood vessel reaches the maximum diastolic state, the microcirculation resistance becomes 0.24 times of the resting state [26], Rn_hyp represents the congestion state, and the coronary artery branch n Load resistance value after microcirculation. As shown in (2–4):

$$\mathrm{R_{n\_hyp}} = 24\% * \mathrm{Rn_{res}} \qquad 2-4$$

In the calculation model, we use the resistance boundary condition to simulate the change of microcirculation resistance. Therefore, the coronary afterload resistance in the hyperemic state is 24% of the static afterload resistance, but the afterload resistance of different patients may be 18% -32% [26].
In order to be able to test whether the microcirculation resistance becomes 0.24 times that of the resting state, we simulated the microcirculation resistance,

and the downstream microcirculation resistance of the diseased branch was adjusted to be based on the basic condition of the coronary artery tree structure model differs in the reduction level (24%, 48%, 72%, 96%).

## 5.6 The calculation of FFR

In the clinical FFR operation, professional clinicians measured the aortic pressure of the enrolled patients, and obtained the pressure pd at the distal end of coronary artery stenosis 3cm [29] of 15 patients through the pressure guide wire. According to the simplified the calculation $\mathrm{FFR} = \frac{Pd}{Pa}$[6]. In the FFR simulation calculation model, when the steady-state calculation model reaches convergence, the pressure at the distal end of the stenosis is extracted, and the CT-based FFR value is obtained using the formula. As is shown in Fig. 4.

## Abbreviations

CFD; computational fluid dynamics, FFRss:a fast calculation method of steady-state fractional flow reserve, CDC:Centers for Disease Control, CVD:cardiovascular disease, CAD:Coronary Artery Disease, RCA:right coronary artery, LAD:left anterior descending (artery), LCx:left circumflex, HR:Heart rate.

## Declarations

### Ethics approval and consent to participate

This study passed the inspection by the medical ethics committee of People's Hospital, Peking University. All participants have signed an informed consent.

### Consent for publication

All patients of this study have agreed to publish. This study passed the inspection by the medical ethics committee of People's Hospital, Peking University. All participants have signed an informed consent.

### Availability of data and materials

The datasets used and/or analysed during the current study are available from the corresponding author on reasonable request.

### Competing interests

The authors declare that there is no conflict of interests of this article.

### Funding

This study was supported by National Natural Science Foundation of China (11832003, 11772016, 11702008), National Key R&D Program of China (7), and Key Project of Science and Technology of Beijing Municipal Education Commission (KZ201810005007). Funding from Support Plan for High-level Faculties in Beijing Municipal Universities (CIT&TCD201804011) and Beijing Excellent Talents Funds (2017000020124G277) are greatly acknowledged.

### Authors' contributions

Jincheng Liu was responsible for modeling, simulation, data analysis and paper preparation.

Xue Wang assisted the hemodynamic simulation.

Junling Ma assisted in data analysis.

Jian Liu was responsible for providing experimental data.

Youjun Liu were responsible for supervision.

### Acknowledgements

This study thanks to the clinical trial data provided by Peking University People's Hospital.

## References

[1] Murphy S, Xu J & Kochanek KD. Deaths: final data for 2010. Natl Vital Stat Rep.2013; 61:1–117.

[2] Dantas AP. Jiménez-Altayó, F . & Vila E. Vascular Aging: Facts and Factors. Frontiers in Physiology. 2012;3:325.

[3] Mortality, G.B.D. and C. Causes of Death, Global, regional, and national age-sex specific all-cause and cause-specific mortality for 240 causes of death, 1990-2013: a systematic analysis for the Global Burden of Disease Study 2013. Lancet. 2015. 385(9963): p. 117-71.

[4] Wong ND, Epidemiological studies of CHD and the evolution of preventive cardiology. Nat Rev Cardiol. 2014. 11(5): p. 276-89.

[5] Pijls NHJ, Fearon WF, Tonino PAL, Siebert U, Ikeno F, Bornschein B , et al. Fractional flow reserve versus angiography for guiding percutaneous coronary intervention in patients with multivessel coronary artery disease: 2-year follow-up of the FAME (Fractional Flow Reserve Versus Angiography for Multivessel Evaluation) study. J Am Coll Cardiol. 2010. 56(3): p. 177-84.

[6] Pijls NH, De Bruyne B, Peels K, Pepijn H, Hans J.R.M, Jozef B, et al. Measurement of fractional flow reserve to assess the functional severity of coronary-artery stenoses. N Engl J Med. 1996;334:1703-8.

[7] Kakouros N, Rybicki FJ, Mitsouras D, Miller JM. Coronary pressure-derived fractional flow reserve in the assessment of coronary artery stenoses. Eur Radiol. 2013;23:958-67.

[8] Michiels V, Eeckhout E, Muller O. Diagnostic Accuracy of Combined Intracoronary Pressure and Flow Velocity Information During Baseline Conditions Adenosine-Free Assessment of Functional Coronary Lesion Severity[J]. Circulation Cardiovascular Interventions, 2012, 5(4):508-14.

[9] De Bruyne B, Sarma J. Fractional flow reserve: a review. Heart 2008;94:949.

[10] Heyndrickx GR, Tóth GG. The fame trials: impact on clinical decision making. Interv Cardiol Rev 2016;1 1:1 16. doi: 10.15420/icr.2016:14:3

[11] Koo BK, Erglis A, Doh JH, Daniels DV , Jegere S , & Kim H S, et al. Diagnosis of Ischemia-Causing Coronary Stenoses by Noninvasive Fractional Flow Reserve Computed From Coronary Computed Tomographic Angiograms Results From the Prospective Multicenter DISCOVER-FLOW (Diagnosis of Ischemia-Causing Stenoses Obtained Via Noninvasive Fractional Flow Reserve) Study. J Am Coll Cardiol. 2011;58:1989-97.

[12] Min JK, Berman DS, Budoff MJ, JafferF A□LeipsicJ□LeonM B□et al. Rationale and design of the DeFACTO (Determination of Fractional Flow Reserve by Anatomic Computed Tomographic Angiography) study. J Cardiovasc Comput. 2011;5:301-9.

[13] Nakazato R, Park HB, Gransar H, Leipsic J A , Budoff M J, & Mancini G , et al. Improved Diagnosis, Discrimination and Reclassification of Ischemia-Causing Lesions by Atherosclerotic Plaque Characteristics and Non-Invasive Fractional Flow Reserve Derived From Coronary CT Angiography. Circulation. 2013;128:A10376.

[14] Taylor CA, Fonte TA, Min K. Computational Fluid Dynamics Applied to Cardiac Computed Tomography for Noninvasive Quantification of Fractional Flow Reserve Scientific Basis. J Am Coll Cardiol. 2013;61:2233-41.

[15] Patel MR. Detecting Obstructive Coronary Disease With CT Angiography and Noninvasive Fractional Flow Reserve. Jama-J Am Med Assoc. 2012;308:1269-70.

[16] Min JK, Leipsic J, Pencina MJ. Diagnostic Accuracy of Fractional Flow Reserve From Anatomic CT Angiography. Jama-J Am Med Assoc. 2012;308:1237-45.

[17] Norgaard BL, Leipsic J, Gaur S, Seneviratne S, Ko BS, & Ito H, et al. Diagnostic Performance of Noninvasive Fractional Flow Reserve Derived From Coronary Computed Tomography Angiography in Suspected Coronary Artery Disease The NXT Trial (Analysis of Coronary Blood Flow Using CT Angiography: Next Steps). J Am Coll Cardiol. 2014;63:1145-55.

[18] Zarins CK, Taylor CA, Min JK. Computed Fractional Flow Reserve (FFTCT) Derived from Coronary CT Angiography. J Cardiovasc Transl. 2013;6:708-14.

[19] Meijs MFL, Cramer MJ, El Aidi H, Doevendans PA. CT fractional flow reserve: the next level in non-invasive cardiac imaging. Neth Heart J. 2012;20:410-8.

[20] Yoon YE, Choi JH, Kim JH, Park KW, Doh J H , & Koo BK,et al. Noninvasive Diagnosis of Ischemia-Causing Coronary Stenosis Using CT Angiography Diagnostic V alue of Transluminal Attenuation Gradient and Fractional Flow Reserve Computed From Coronary CT Angiography Compared to Invasively Measured Fractional Flow Reserve. Jacc-Cardiovasc Imag. 2012;5:1088-96.

[21] Sdringola S, Johnson NP, Kirkeeide RL, Cid E, Gould KL. Impact of unex-pected factors on quantitative myocardial perfusion and coronary flow reserve in young, asymptomatic volunteers. JACC Cardiovasc Imaging 201 1;4:402–12.

[22] Wilson RF, Wyche K, Christensen BV, Zimmer S, Laxson DD.Effects of adenosine on human coronary arterial circulation. Circulation1990;82:1595–606.

[23] Sankaran S, Kim HJ, Choi G, Taylor CA. Uncertainty quantification in coronary blood flow simulations: Impact of geometry, boundary conditions and blood viscosity. Journal of Biomechanics. 2016;49(12):2540-7.

[24] Wang W, Tang D, Mao B, Li B, Liu Y. A Fast-Fractional Flow Reserve Simulation Method in A Patient with Coronary Stenosis Based on Resistance Boundary Conditions. Computer Modeling in Engineering & Sciences, 2018, 116(2):163-173.

[25] Sharma P, Itu L,Zheng X,Kamen A,D Comaniciu D. A framework for personalization of coronary flow computations during rest and hyperemia. Conf Proc IEEE Eng Med Biol Soc, 2012. 2012: p. 6665-8.

[26] Kim HJ, Vignon- Clementel IE Coogan JS Figueroa CA KE Jansen , Taylor CA, Patient-specific modeling of blood flow and pressure in human coronary arteries. Ann Biomed Eng, 2010. 38(10): p. 3195-209.

[27] Olufsen MS. Structured tree outflow condition for blood flow in larger systemic arteries. Am J Physiol Circ Physiol 1999;276.

[28] Itu, L, Sharma P,Suciu C,Moldoveanu F,Comaniciu D, Personalized blood flow computations: A hierarchical parameter estimation framework for tuning boundary conditions. Int J Numer Method Biomed Eng, 2017. 33(3).

[29] Solecki M, Kruk M, Demkow M, Schoepf UJ, Reynolds MA, Wardziak Ł, et al. What is the optimal anatomic location for coronary artery pressure mea- surement at CT-derived FFR? J Cardiovasc Comput Tomogr 2017;1 1:397–403.

[30] Alrifai A, Kabach M, Nieves J, Pino J, Chait R. Microvascular coronary artery disease: review article. US Cardiol Rev 2017;1. doi: 10.15420/usc.2017:27:1

[31] Faria D C , Lee J M , Hoef T , Rentería HM, Escaned J. Age and Functional Relevance of Coronary Stenosis: a Post-Hoc Analysis of the ADVISE II Trial[J]. EuroIntervention: journal of EuroPCR in collaboration with the Working Group on Interventional Cardiology of the European Society of Cardiology, 2021.

## Figures

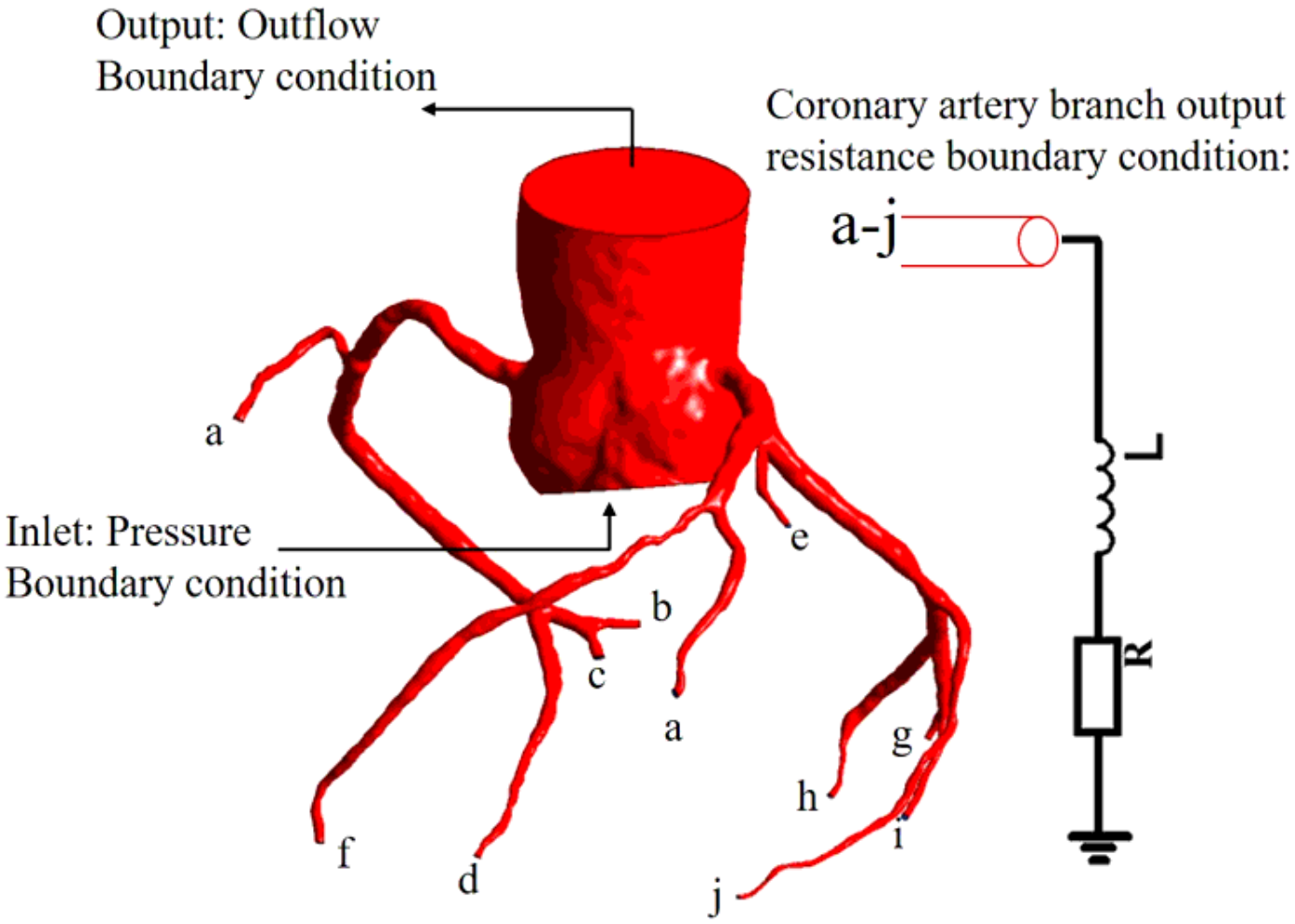


**Figure 1**

FFRss model structure diagram. The coronary artery is a three-dimensional model, the microcirculation part of the coronary artery is an 0D circuit model, and 3D and 0D are coupled for calculation.

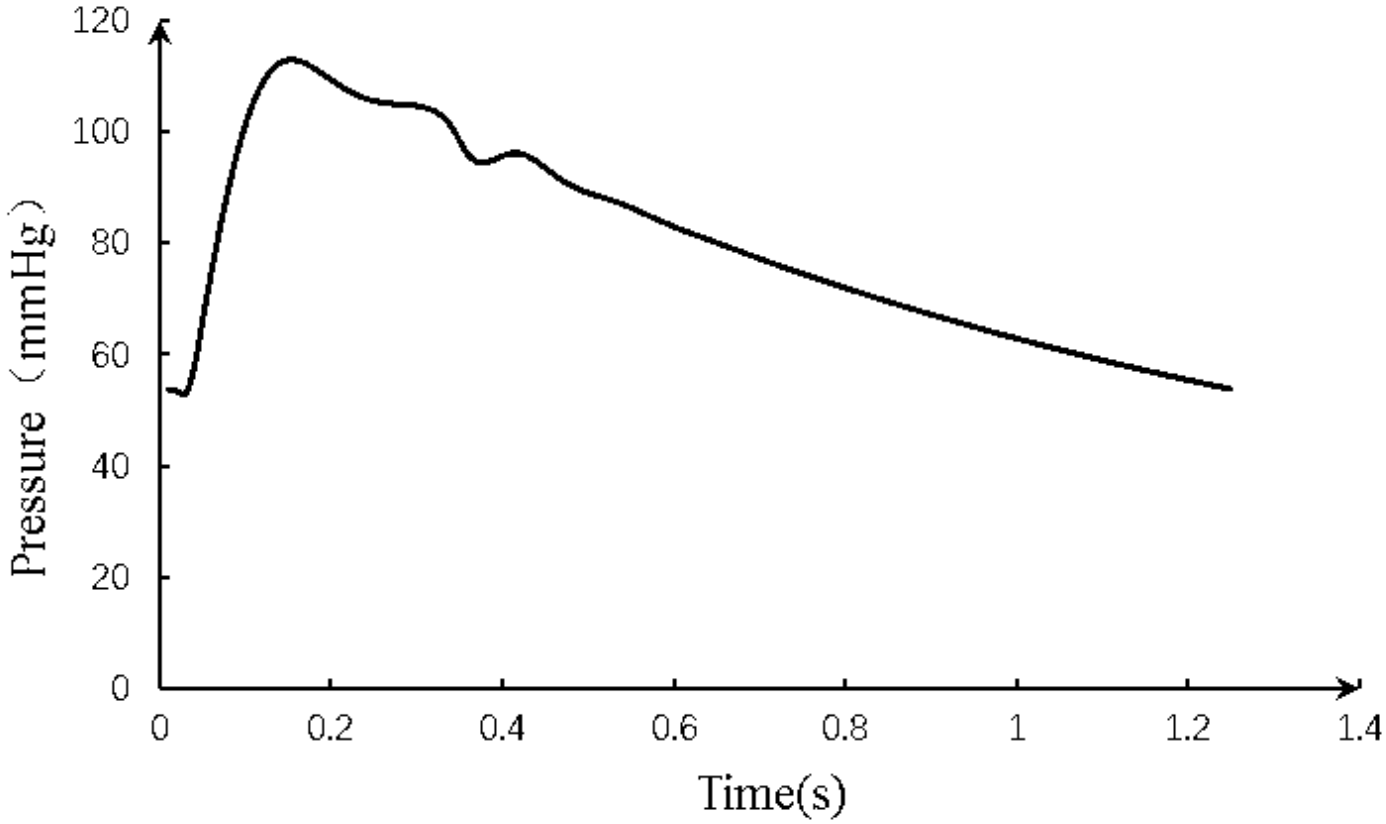


**Figure 2**

Schematic diagram of the clinically measured aortic pressure waveform (a single cycle).

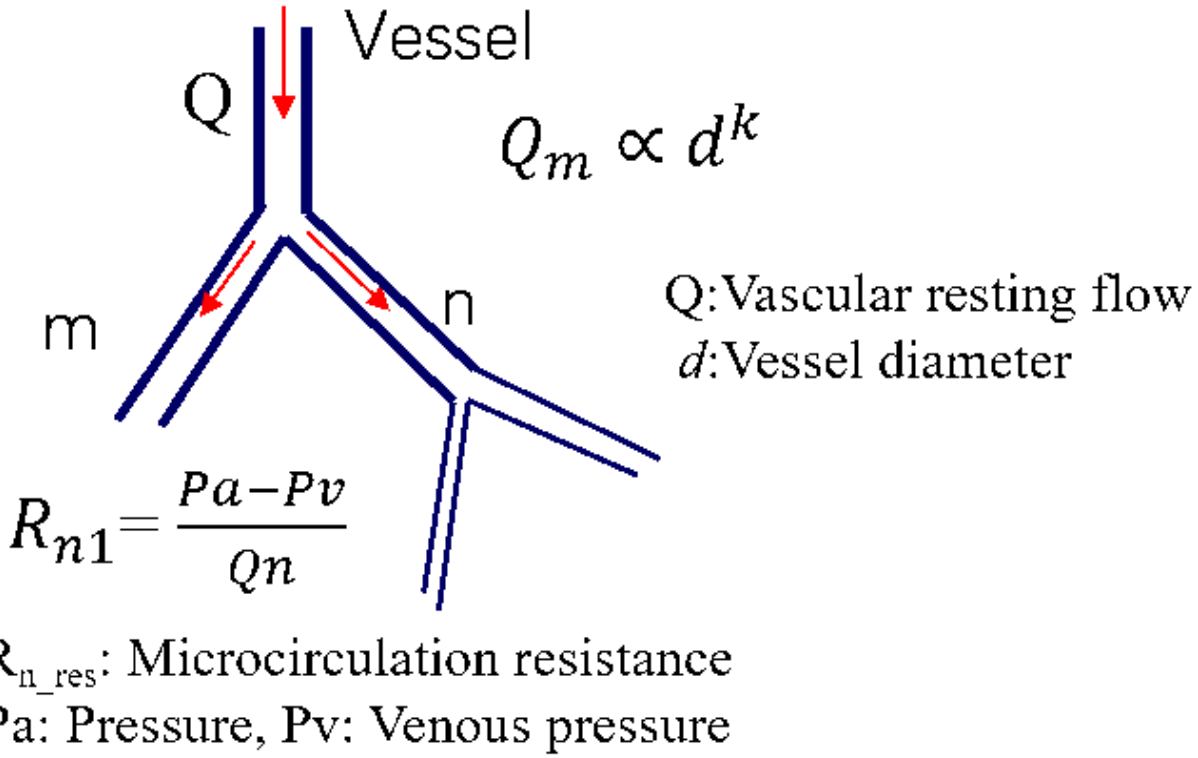

## Figure 3

The allometric scaling law calculates the microcirculation resistance. (The bifurcation ideal blood vessel model calculates the microcirculation resistance)

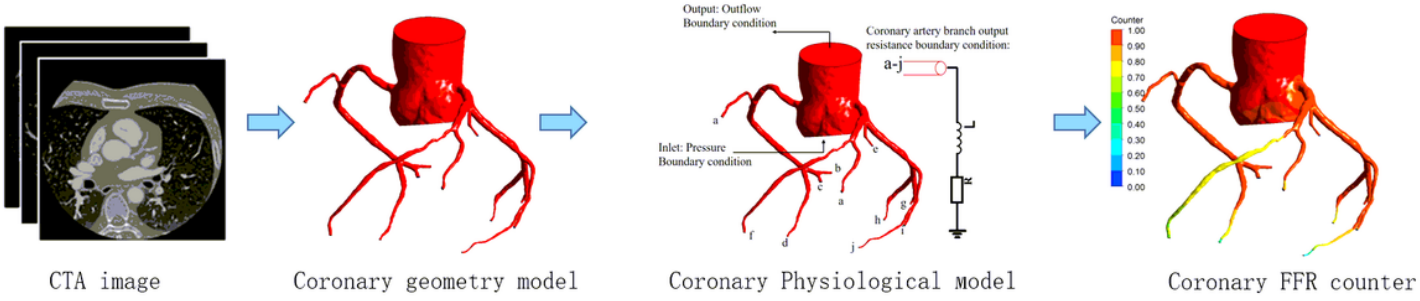


## Figure 4

The chart of FFRss non-invasive calculation of FFR. A: Obtains the CTA image for 3D automatic reconstruction. B: The geometric model established based on the CTA image. C: The constructed physiological model for multi-scale coupling calculation. D: The FFR numerical cloud image calculated by the coronary artery model.

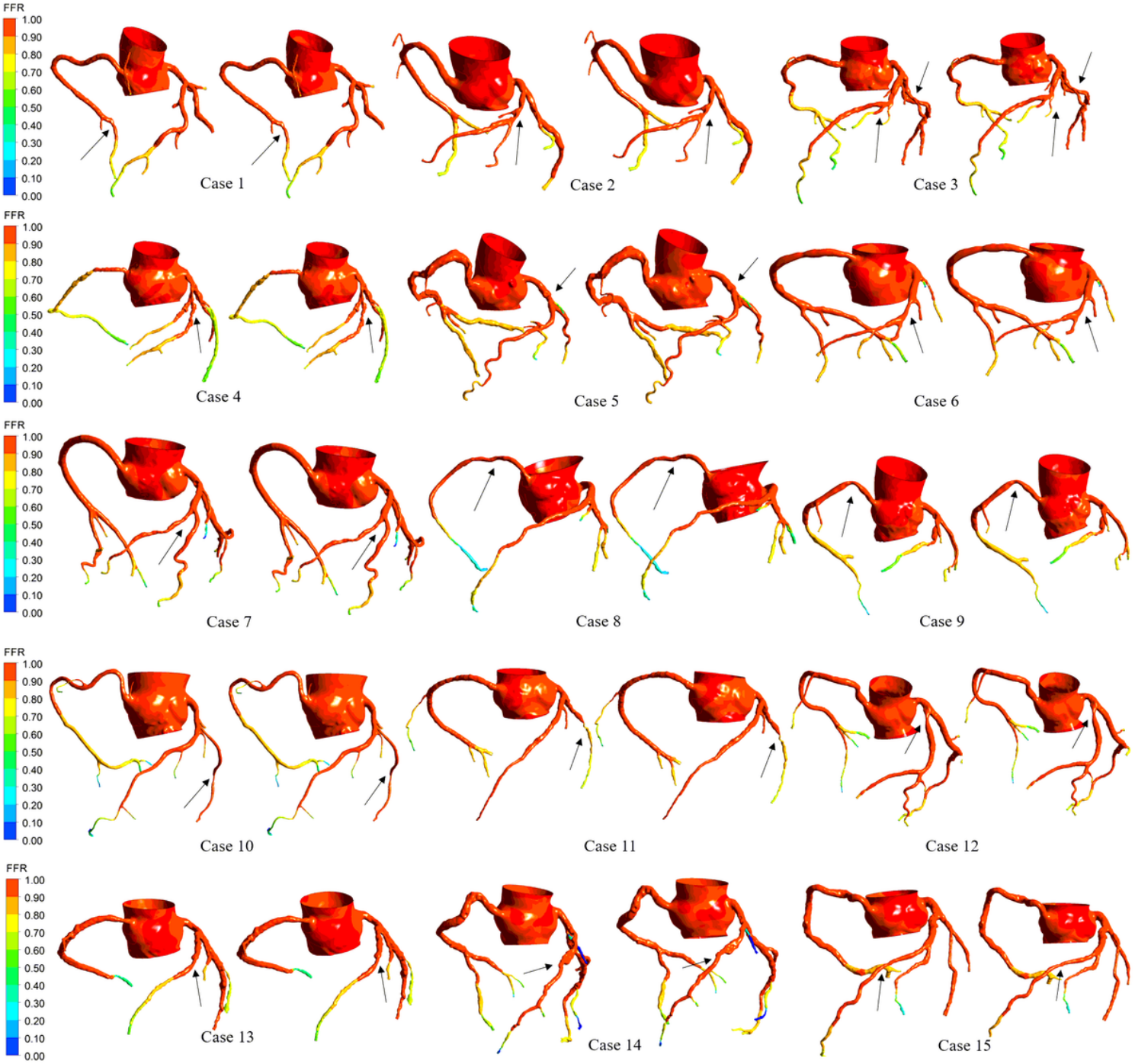


## Figure 5

FFR contours of 15 patients under two different aortic pressure boundary conditions.